Towards a Finite Element Calculation of Acoustical Amplitudes in HID Lamps

Bernd Baumann[*,1], *Marcus Wolff*[1], *John Hirsch*[2], *Piet Antonis*[2], *Sounil Bhosle*[3] *and Ricardo Valdivia Barrientos*[4]
[1] *Hamburg University of Applied Sciences, Germany*
[2] *Philips Lighting, Eindhoven, The Netherlands*
[3] *Université de Toulouse and CNRS, LAPLACE, Toulouse, France*
[4] *National Institute of Nuclear Research, Salazar, Ocoyoacac, Mexico*
[*] *Berliner Tor 21, 20099 Hamburg, Germany, email: bernd.baumann@haw-hamburg.de*

Abstract: High intensity discharge lamps can experience flickering and even destruction, when operated at high frequency alternating current. The cause of these problems has been identified as acoustic resonances inside the lamp's arc tube. Here, a finite element approach for the calculation of the acoustic response function is described. The developed model does not include the plasma dynamics.

Keywords: HID lamp, acoustic resonance, energy efficiency

1 Introduction

Reduction of energy consumption is one of the most important issues for modern societies. Together with fuel efficient vehicles and energy efficient buildings, lighting has a high energy saving potential. To save energy in the field of indoor lighting, Europe, Australia, and New Zealand have all passed laws prohibiting the sale of traditional light bulbs. High intensity discharge (HID) lamps offer here an interesting alternative as they are highly efficient light sources. Further improvement is also deemed to be a possibility. For outdoor lighting HID lamps are already used to a large extent (streets, roadways, stadiums, etc.).

In HID lamps light is generated by a gas discharge inside a confinement made from ceramics or quartz called arc tube or burner. The gas mixture inside the arc tube is usually mercury with some additives such as metal halides (NaI, TlI, etc.). It is heated, and therefore partially ionized, by maintaining an electrical current between two electrodes. The ionized gas forms the light emitting arc (Figure 1, left). Details on the working principle of HID lamps can be found elsewhere [1, 2, 3].

To prevent demixing of gas components inside the burner, the lamp is operated at alternating current. As a result of this periodic heating, an acoustic wave with the modulation frequency of the power in the discharge is generated. It propagates toward the walls where it is damped and reflected. Incident and reflected waves interfere which leads to the development of standing acoustic waves. At certain frequencies resonances form. The standing waves interact with the discharge arc [4] and are responsible for its distortion and instability (Figure 1, right). These take the form of flickering light, reduction of the lamp's lifetime or even destruction of the lamp. In order to further improve HID lamps it is necessary to understand and control the acoustic resonance phenomenon.

In this article, we derive a finite element (FE) model that describes the generation of acoustic resonances which are responsible for the onset of acoustic streaming. This model does not include the plasma dynamics, and is based on a simplified geometry. Static temperature and power distributions are used. In a forthcoming article we plan to take into account plasma dynamics. The calculations have been performed using COMSOL Multiphysics with the default parameter settings [5].

2 Theory

In previous COMSOL conferences some of the authors of this paper reported on the calculation of the pressure inside the resonator of photoacoustic sensors [6, 7], see also [8, 9]. Here we describe how an equivalent method can be applied to estimate the strength of acoustic resonances inside the burner of HID lamps.

The starting point is the inhomogeneous Helmholtz Equation for the acoustic pressure

$$\vec{\nabla}\left(\frac{1}{\rho}\vec{\nabla}p\right)+\frac{\omega^2}{\rho c^2}p=\mathrm{i}\omega\frac{\gamma-1}{\rho c^2}\mathcal{H}\,, \qquad (1)$$

where γ denotes the ratio of the specific heat at

constant pressure c_p to the specific heat at constant volume c_V. $\mathcal{H}(\vec{r},\omega)$ constitutes the Fourier transform of the power density deposited in the gas.

Contrary to the case of the photoacoustic sensor, the temperature T in the burner is not constant, but space dependent. The density ρ of the burner filling and the speed of sound c become a space dependency as well. In this work it is assumed that the relation of T and ρ is described by the ideal gas law and c and T are related through $c = \sqrt{\gamma R_\mathrm{m} T/M}$ (gas constant R_m, molar mass M).

Loss is accounted for via loss factors. The surface loss factor associated with the j-th acoustical eigenfrequency ω_j of the burner (volume V_B) resulting from shear stress is calculated from the surface integral

$$L_j^{(\mathrm{s}_\eta)} = \frac{1}{\sqrt{2\omega_j}\omega_j^2 V_\mathrm{B}} \int_{S_\mathrm{B}} \sqrt{\frac{\eta}{\rho}}\, c^2 \left|\vec{\nabla}_\mathrm{t}\, p_j\right|^2 \mathrm{d}S. \tag{2}$$

$\vec{\nabla}_\mathrm{t}\ p_j$ denotes the component of the pressure gradient tangential to the burner wall and the integral has to be taken over the entire surface of the burner. Surface loss due to heat conduction can be calculated from the similar integral

$$L_j^{(\mathrm{s}_\kappa)} = \frac{\gamma-1}{\sqrt{2c_p\omega_j}V_\mathrm{B}} \int_{S_\mathrm{B}} \sqrt{\frac{\kappa}{\rho}} \left|p_j\right|^2 \mathrm{d}S. \tag{3}$$

The integrals contain the associated transport coefficients η (coefficient of viscosity) and κ (coefficient of heat conduction), respectively.

Equation (3) is derived under the assumption that the thermal conductivity of the wall is very large compared to the thermal conductivity of the gas. A rough estimation of the ratio of the thermal conductivities results in $\kappa_\mathrm{wall}/\kappa_\mathrm{plasma} = \mathcal{O}(50)$. This is considered to be large, and therefore justifies the use of Equation (3).

The volume loss due to shear stress is described by

$$L_j^{(\mathrm{v}_\eta)} = \frac{4}{3\rho c^2} \sum_i \omega_i \left(\frac{A_i}{A_j}\right)^* \frac{1}{V_\mathrm{B}} \int_{V_\mathrm{B}} \eta\, p_i^* p_j \mathrm{d}V. \tag{4}$$

This equation is derived by following the reasoning of Morse and Ingard [10], Kreuzer [11] and considering that $\rho c^2 = \text{const}$. If η were constant, as is the case for photoacoustic sensors, the above sum is reduced to a single term due to the orthogonality of the eigenmodes p_j.

In order to allow an estimation of the loss factor, Equation (4), we describe the viscosity as a sum of a constant and a space dependent part:

$$\eta(\vec{r}) = \bar{\eta} + \hat{\eta}(\vec{r}). \tag{5}$$

$\bar{\eta}$ is chosen to be the mean value of the minimum and maximum viscosity inside the burner. This leads to

$$L_j^{(\mathrm{v}_\eta)} = \frac{4}{3}\,\frac{\bar{\eta}}{\rho c^2}\,\omega_j + \text{corrections}. \tag{6}$$

For volume loss due to thermal conduction we proceed in the same way. Splitting the coefficient of thermal conduction

$$\kappa(\vec{r}) = \bar{\kappa} + \hat{\kappa}(\vec{r}) \tag{7}$$

leads to

$$L_j^{(\mathrm{v}_\kappa)} = \frac{(\gamma-1)\bar{\kappa}}{c_p\rho c^2}\,\omega_j + \text{corrections}. \tag{8}$$

In order to check if the correction terms in Equations (6) and (8) are negligible, we make the following estimation: ignoring these corrections and using the values of Table 1 the two volume loss factors can be calculated. In this approximation volume loss scales linearly with frequency:

$$L_j^{(\mathrm{v})} = L_j^{(\mathrm{v}_\kappa)} + L_j^{(\mathrm{v}_\kappa)} \sim \omega_j. \tag{9}$$

Critical damping corresponds to $L_j^{(\mathrm{v})} = 2$ and, therefore, occurs at a frequency $f_\mathrm{crit} \approx 1$ GHz. It is very unlikely that the correction terms would change f_crit by orders of magnitude and it is reasonable to disregard the corrections in the volume loss formulas for the frequency range considered in this paper.

The solution of the Helmholtz equation can be expressed as a superposition of the normalized eigenmodes

$$p(\vec{r},\omega) = \sum_j A_j(\omega) p_j(\vec{r}), \tag{10}$$

where the contribution of a certain mode is determined by the frequency dependent amplitudes $A_j(\omega)$. These amplitudes exhibit a Lorentzian profile according to

$$A_j(\omega) = \mathrm{i}\frac{\mathcal{A}_j\omega}{\omega^2 - \omega_j^2 + \mathrm{i}\omega\omega_j L_j}. \tag{11}$$

The excitation amplitude $\mathcal{A}_j$ corresponding to the j-th mode is calculated from a scalar product of the mode and the power density profile

$$\mathcal{A}_j = \frac{(\gamma-1)}{V_\mathrm{B}} \int_{V_\mathrm{B}} p_j^* \mathcal{H}\, \mathrm{d}V. \tag{12}$$

Details about the theoretical framework described in this section can be found elsewhere [12].

3 Results

Using the equations presented in the previous section, we performed an FE calculation of the response function of the acoustic pressure inside the burner of an HID lamp. The burner is assumed to be of cylinder shape (radius $R = 3.425\ \mathrm{mm}$, length $L = 7\ \mathrm{mm}$). The frequency range from $10\ \mathrm{kHz}$ to $1\ \mathrm{MHz}$ is covered in 50 Hz-steps. In order to restrict memory requirements and CPU time, the simulation has been performed as a two-dimensional axisymmetric model without nontrivial azimuthal modes. Due to the large frequencies involved it is necessary to use about 400 modes and a very fine FE mesh.

The following assumptions have been made (all physical constants are collected in Table 1): The power density is assumed to be of Gaussian profile

$$\mathcal{H}(\vec{r}) = \mathcal{H}_0 \exp\left(-2\left(\frac{r_\perp}{w}\right)^2\right), \qquad (13)$$

where $r_\perp$ is the distance from the burner axis and w is the radius of the power profile. The coefficient $\mathcal{H}_0$ has been chosen arbitrarily since its determination requires the modeling of the plasma dynamics. Consequently, all following pressure results are relative.

The temperature distribution inside the burner is described by

$$T(r_\perp) = T_a - (T_a - T_w)\left(\frac{r_\perp}{R}\right)^2. \qquad (14)$$

For the description of the temperature dependency of the viscosity we use Sutherland's law [13]

$$\eta = \eta_0 \left(\frac{T}{T_0}\right)^{3/2} \frac{T_0 + T_\mathrm{S}}{T + T_\mathrm{S}}. \qquad (15)$$

and for the coefficient of thermal conduction we use [14]

$$\kappa = \kappa_0 \exp\left(\frac{T}{T_1} + \arctan\left(\frac{T - T_2}{T_3}\right) - 1.3\right). \qquad (16)$$

In order to quantify the acoustic resonance phenomenon, the acoustic pressure as a function of the driving frequency (response function) has been calculated. The shape of this response function depends on the location for which it is determined. To judge the overall response, two extreme locations inside the burner have been chosen (center of burner, edge of burner). The resulting response function for these locations is depicted in Figures 2 and 3. Figure 2 also shows the excitation amplitude according to Equation (12) and the total loss factor. It becomes evident from this figure that a large excitation amplitude is a prerequisite for a strong resonance. It has been checked that large excitation amplitudes appear for purely radial modes only. Figure 4 (left) shows the power density of the discharge arc together with two different radial modes (middle part and right). It is easy to understand that the overlap integral of Equation (12) for the mode depicted in the middle of Figure 4 and the power density is large. On the other hand, the overlap integral of the power density and the highly excited radial mode depicted on the right is small due to cancellations of positive and negative contributions. It is important to be aware of the fact that the figures show the absolute value of the pressure $|p|$ and that neighboring antinodes correspond to different signs of the pressure. The decrease of the excitation amplitude and the increase of loss with frequency explain the decrease in the resonance amplitudes with increasing frequency.

Therefore, the symmetries of burner geometry and power density profile allow for the efficient excitation of radial modes. Longitudinal modes, on the other hand, cannot be excited under the considered conditions, since the overlap integral (12) of power density and longitudinal modes is exactly zero. Strictly speaking, pure longitudinal modes do not even exist in the arc tube of an HID lamp, due to the space dependency of the speed of sound. As a result nodes and antinodes are no longer plane but curved (see Figure 5, left). The excitation amplitudes of the nonradial modes of Figure 5 are small but not identical to zero.

As mentioned above, in this investigation only trivial azimuthal modes are considered. Still, it is worthwhile to mention that nontrivial azimuthal modes cannot be excited due to the symmetry of the model.

4 Conclusions

The aim of our work was to calculate the acoustical response function inside the arc tube of an HID lamp, starting from a simplified description of the plasma. It has been found that the cylinder symmetry of the geometry, and of all physical coefficient profiles, results in resonances, which are connected to purely radial modes. Despite the simplicity of the model, first experimental results show good agreement with the calculated amplitude.

The model described in this article is intended to serve as a starting point for a more comprehensive model, which includes the plasma dynamics. Also, a realistic description of HID lamps requires a three-dimensional model. Such a model would allow optimization of the lamps with regard the acoustic resonance problem.

References

[1] J. F. Waymouth. *Electric discharge lamps*. M.I.T. Press, 1971.

[2] J. J. De Groot and J. A. J. M. Van Vliet. *The High-pressure Sodium Lamp*. Scholium Intl, 1986.

[3] P. Flesch. *Light and light sources: high-intensity discharge lamps*. Springer, 2006.

[4] F. Afshar. The theory of acoustic resonance and acoustic instability in hid lamps. *LEUKOS*, 20(1):27–38, 2008.

[5] COMSOL-Homepage: www.comsol.com.

[6] B. Baumann, B. Kost, H. Groninga and M. Wolff. Eigenmodes of Photoacoustic T-cells. Proceedings FEMLAB Conference, Frankfurt, 2005.

[7] B. Baumann, M. Wolff, B. Kost and H. Groninga. Calculation of Quality Factors and Amplitudes of Photoacoustic Resonators. Proceedings FEMLAB Conference, Frankfurt, 2006.

[8] B. Baumann, B. Kost, H. Groninga and M. Wolff. Eigenmode Analysis of Photoacoustic Sensors via Finite Element Method. *Rev. Sci. Instrum.*, 77, 044901, 2006.

[9] B. Baumann, M. Wolff, B. Kost, and H. Groninga. Finite element calculation of photoacoustic signals. *Applied Optics*, 46:1120–1125, 2007.

[10] P. M. Morse and K. U. Ingard. *Theoretical Acoustics*. Princeton University Press, 1987.

[11] L. B. Kreuzer. The physics of signal generation and detection. In Y.-H. Pao, editor, *Optoacoustic Spectroscopy and Detection*, pages 1–25, London, 1977. Academic.

[12] B. Baumann, M. Wolff, B. Kost, and H. Groninga. Solving a coupled field problem by eigenmode expansion and finite element method. *International Journal of Multiphysics*, 1(3):303–315, 2007.

[13] W. Sutherland. The viscosity of gases and molecular force. *Philosophical Magazine*, 36(5):507–531, 1893.

[14] U. Niemann H. Giese, Th. Kruecken and F. Noertemann. Understanding hid lamp properties. *Proceedings of SPIE*, 4775:1–21, 2002.

specific heat capacity at constant pressure	$c_p = 114\ \mathrm{J/kg\,K}$
adiabatic exponent	$\gamma = 1.66667$
pressure of mercury	$P_{\mathrm{Hg}} = 18\ \mathrm{hPa}$
temperatures:	
of burner wall	$T_w = 1300\ \mathrm{K}$
on axis	$T_a = 5000\ \mathrm{K}$
Sutherland's constant	$T_{\mathrm{S}} = 850\ \mathrm{K}$
	$T_0 = 273\ \mathrm{K}$
	$T_1 = 4000\ \mathrm{K}$
	$T_2 = 5200\ \mathrm{K}$
	$T_3 = 330\ \mathrm{K}$
viscosities:	
	$\eta_0 = 2.25 \cdot 10^{-5}\ \mathrm{Pa\,s}$
	$\bar{\eta} = 2.3 \cdot 10^{-4}\ \mathrm{Pa\,s}$
coefficients of heat conduction:	
	$\kappa_0 = 0.375\ \mathrm{W/m\,K}$
	$\bar{\kappa} = 0.12\ \mathrm{W/m\,K}$
molar mass of mercury	$M_{\mathrm{Hg}} = 200\ \mathrm{kg/kmol}$
radius of discharge arc	$w = 1\ \mathrm{mm}$

Tab. 1: Physical quantities used in this article.

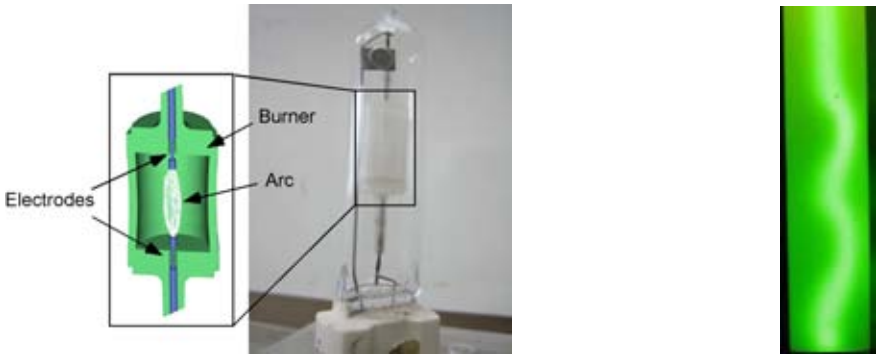

Fig. 1: Structure of HID lamp (left) and by acoustic resonances disturbed arc (right).

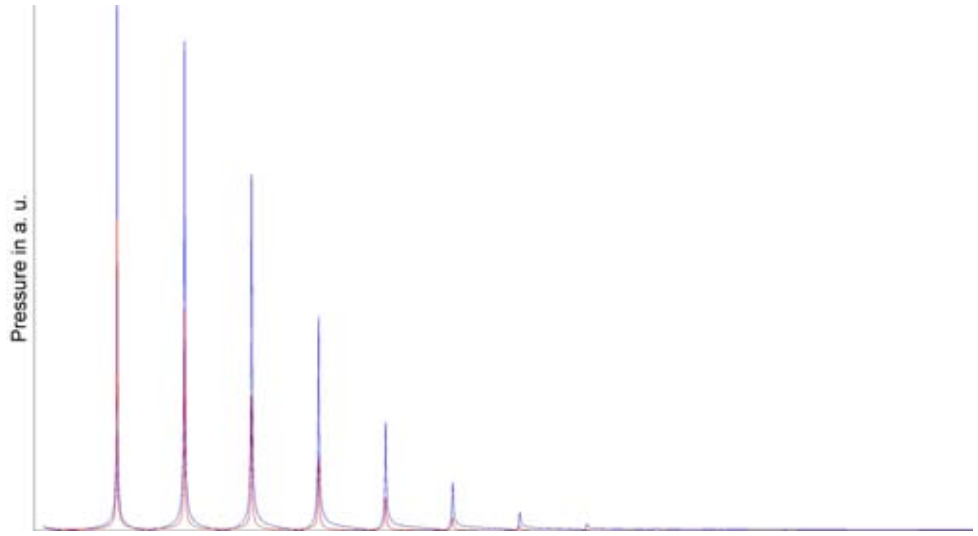

Fig. 2: Response function in arbitrary units at two different locations inside the arc tube (top), logarithm of excitation amplitudes according to Equation (12) in arbitrary units (middle) and total loss factor times 10^3 (bottom) as function of the frequency in Hz.

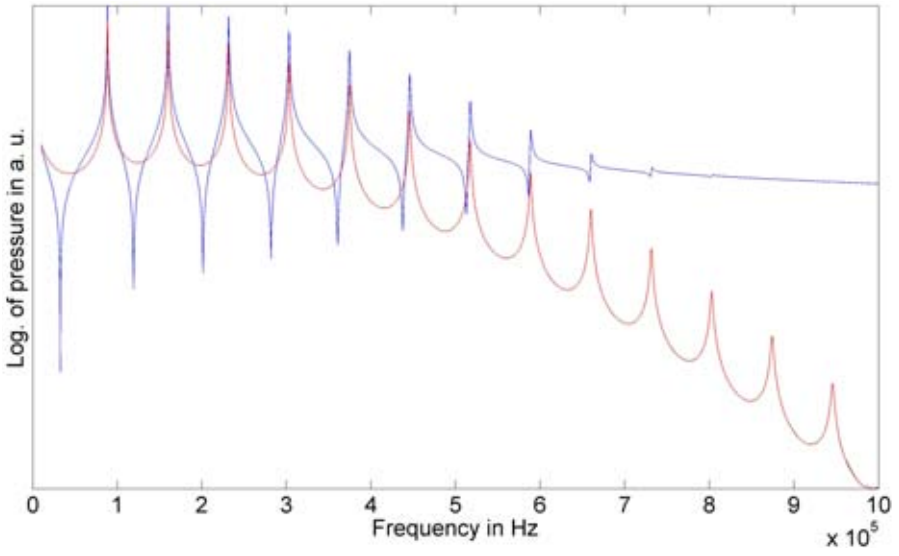

Fig. 3: Logarithm of response function in arbitrary units at two different locations inside the arc tube as function of the frequency in Hz. The dashed line depicts the pressure at the center and the full line at an outer corner of the burner (see Figure 4).

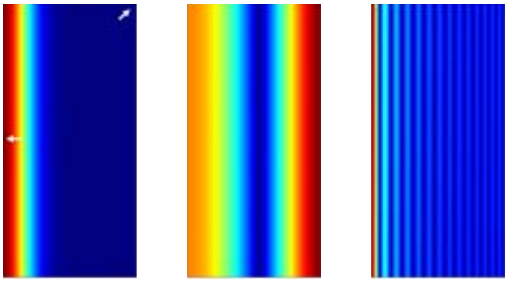

Fig. 4: Left: Power density according to Equation (13) for $w = 1\ \mathrm{mm}$. The arrows indicate the locations where the response functions have been calculated. Middle and right: Absolute value of acoustic pressure $|p|$ for two radial modes (eigenfrequencies $88.33\ \mathrm{kHz}$ and $1014\ \mathrm{kHz}$, respectively). Blue indicates nodes whereas red indicates antinodes. The left edge is the location of the cylinder axis.

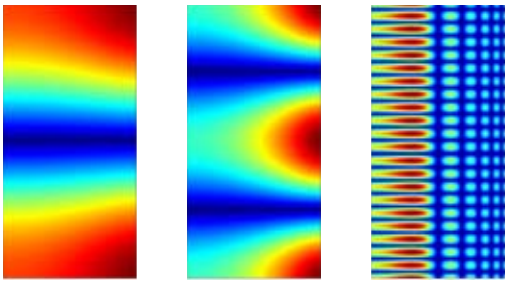

Fig. 5: Absolute value of acoustic pressure $|p|$ for some modes (eigenfrequencies $33.11\ \mathrm{kHz}$, $64.71\ \mathrm{kHz}$ and $866.5\ \mathrm{kHz}$ respectively). Blue indicates nodes whereas red indicates antinodes. The left edge is the location of the cylinder axis. Because of the space dependency of the speed of sound even in a cylinder only approximate longitudinal modes are possible (left). Despite the short wavelength of the high order mode on the right the resolution of the FE-mesh is sufficient to represent the mode accurately.